

1 Characterization of the Saffron Derivative Crocetin as an  
2 Inhibitor of Human Lactate Dehydrogenase 5 in the  
3 Antiglycolytic Approach against Cancer

4  
5 *Carlotta Granchi,<sup>a</sup> Serena Fortunato<sup>a</sup> Serena Meini,<sup>a</sup> Flavio Rizzolio,<sup>c</sup> Isabella Caligiuri,<sup>d</sup>*  
6 *Tiziano Tuccinardi,<sup>a,e</sup> Hyang Yeon Lee,<sup>b</sup> Paul J. Hergenrother,<sup>b</sup> Filippo Minutolo,<sup>a,e,\*</sup>*

7  
8 <sup>a</sup> Dipartimento di Farmacia, Università di Pisa, Via Bonanno 6 and 33, 56126 Pisa, Italy.

9 <sup>b</sup> Department of Chemistry, University of Illinois at Urbana-Champaign, 600 S. Mathews, Urbana,  
10 Illinois 61801, USA.

11 <sup>c</sup> Dipartimento di Scienze Molecolari e Nanosistemi, Università Ca'Foscari, Venezia, Italy.

12 <sup>d</sup> Division of Experimental and Clinical Pharmacology, Department of Molecular Biology and  
13 Translational Research, National Cancer Institute and Center for Molecular Biomedicine, Aviano  
14 (PN), Italy

15 <sup>e</sup> Centro Interdipartimentale di Ricerca "Nutraceutica e Alimentazione per la Salute", Università di  
16 Pisa, Via del Borghetto 80, 56124 Pisa, Italy.

17 AUTHOR INFORMATION

18 **Corresponding Author**

19 \*Corresponding author phone: +39 050-2219557; fax +39 050-2210680; e-mail:

20 [filippo.minutolo@unipi.it](mailto:filippo.minutolo@unipi.it)

21  
22 **Title running header:** Crocetin inhibits LDH in glycolytic cancer cells

23 **ABSTRACT**

24 Inhibition of lactate dehydrogenase (LDH) represents an innovative approach to tackle cancer  
25 because this peculiar glycolytic metabolism is characteristic of most invasive tumor cells. An  
26 investigation into the biological properties of saffron extracts led to the discover of their LDH-  
27 inhibition properties. In particular, the most important saffron components, crocetin, was found to  
28 inhibit LDH ( $IC_{50} = 54.9 \pm 4.7 \mu\text{M}$ ). This carotenoid was independently produced by chemical  
29 synthesis, and its LDH-inhibition properties manifested via its antiproliferative activity against two  
30 glycolytic cancer cell lines (A549 and HeLa,  $IC_{50} = 114.0 \pm 8.0$  and  $113.0 \pm 11.1 \mu\text{M}$ , respectively).  
31 The results described in this article suggest that saffron may be a helpful alimentary component in  
32 the prevention of cancer that potentially contributes to the efficacy of approved cancer therapies.

33

34 **KEYWORDS**

35 • Saffron;

36 • cancer;

37 • crocetin;

38 • lactate dehydrogenase;

39 • glycolysis

40

## 41 INTRODUCTION

42 Inhibition of lactate dehydrogenase (LDH) as a potential anticancer strategy is rationalized via Otto  
43 Warburg's observation that cancer cells rapidly internalize and consume glucose to survive, which in  
44 turn produces large amounts of lactate.<sup>1</sup> In the last decade, a great interest was directed towards the  
45 discovery of antiglycolytic agents capable of interfering with the glycolytic metabolism of cancer  
46 cells.<sup>2,3</sup> In this context, the human homotetrameric isoform 5 of lactate dehydrogenase (*h*LDH-5),  
47 composed of four A subunits, is considered a strategic target to selectively disrupt the metabolism of  
48 cancer cells. Moreover, *h*LDH-5 is overexpressed in many types of tumours. *h*LDH-5 catalyzes the  
49 last step of glycolysis - the reversible reduction of pyruvate to lactate via the simultaneous oxidation  
50 of NADH to NAD<sup>+</sup>. Considering the essential role of this enzyme in the regeneration of NAD<sup>+</sup> and  
51 continuation of glycolysis, we hypothesized its inhibition should lead to cancer cell death by  
52 starvation. Individuals that lack of *h*LDH-5 experience myoglobinuria after intense anaerobic  
53 exercise yet are healthy under ordinary circumstances. Therefore, we hypothesize that the inhibition  
54 of *h*LDH-5 is a potentially safe approach to treating cancer that will avoid the deleterious side-effects  
55 associated with traditional chemotherapy.<sup>4</sup> Previously, *h*LDH-5 was silenced with *si*RNA, resulting  
56 in an evident decrease in cancer cell proliferation and migration.<sup>5</sup> These results laid the groundwork  
57 for the development and the synthesis of many small molecules as *h*LDH-5 inhibitors and several  
58 proved to be potent inhibitors both *in vitro* and *in vivo*.<sup>6</sup> However, the search for new potent inhibitors  
59 remains a challenging goal, since the cavity of the enzyme comprises both a cofactor (NADH)- and  
60 a substrate (pyruvate)-binding pocket. The substrate-binding site is very narrow, polar, and possesses  
61 many positively charged residues, whereas, the cofactor binding region is quite extended since NADH  
62 binds to the enzyme with the nicotinamide and adenosine portions at opposite ends of this site.

63 Several natural products have been identified as *h*LDH-5 inhibitors. One of the first examples is  
64 represented by the natural derivative gossypol (Figure 1), which is extracted from the cotton seeds of  
65 the *Gossypium* species. Gossypol was initially studied as an antimalarial agent, due to its inhibitory

66 activity of the *Plasmodium falciparum* isoform of LDH (*pf*LDH). However, this compound proved  
67 to be a non-selective competitive inhibitor of LDH relative to NADH through its inhibition of the  
68 human LDH isoforms. Additionally, the high toxicity of gossypol (including cardiac arrhythmias,  
69 renal failure, muscle weakness and even paralysis) hampered its further development as an anticancer  
70 agent.<sup>7</sup> Later, the flavonoid epigallocatechin<sup>8</sup> (Figure 1) and the fungal metabolite panepoxydone<sup>9</sup>  
71 (Figure 1) exerted an indirect inhibitory effect on *h*LDH-5 by reducing its expression in cancer cells.  
72 Conversely, the  $\alpha,\beta$ -unsaturated aldehyde 4-hydroxy-2-nonenal (Figure 1), which naturally forms  
73 upon oxidation of unsaturated fatty acids, covalently binds the enzyme and blocks its activity.<sup>10</sup> The  
74 recently identified *h*LDH-5 inhibitor penta-1,2,3,4,6-*O*-galloyl- $\beta$ -D-glucose (Figure 1), a component  
75 of *Rhus Chinensis* gallnut extract, directly inhibits the enzyme via competitive displacement of the  
76 cofactor NADH.<sup>11</sup> Galloflavin (Figure 1), a compound formed via autooxidation of the natural  
77 compound gallic acid, was identified by virtual screening of compounds from National Cancer  
78 Institute dataset and proved to inhibit both *h*LDH-5 and *h*LDH-1 with  $K_i$  values in the micromolar  
79 range and retard cancer cell growth.<sup>12</sup> Luteolin 7-*O*- $\beta$ -D-glucopyranoside (Figure 1) isolated from  
80 *Phlomis kurdica*, inhibits *h*LDH-5 with an  $IC_{50}$  value in the micromolar range. It was shown to be  
81 competitive with NADH; a conclusion supported by modelling studies.<sup>13</sup> Moreover, a high-  
82 throughput screening of medicinal plants identified some natural extracts, such as Chinese Gallnut  
83 (*Melaphis chinensis gallnut*), Bladderwrack (*Fucus vesiculosus*), Kelp (*Laminaria Japonica*) and  
84 Babul (*Acacia Arabica*) that showed *h*LDH-5  $IC_{50}$  values lower than 0.001 mg/ml, although the  
85 individual chemical constituents responsible for the activity were not isolated.<sup>14</sup>  
86 Given that a growing number of natural products have demonstrated the ability to directly and  
87 indirectly *h*LDH-5, we screened a large panel of natural products that are mostly found in alimentary  
88 sources for the purpose of identifying new natural products as food-derived *h*LDH-5 inhibitors. As  
89 such, we sought to identify a possible nutraceutical strategy to produce safe antiglycolytic effects that  
90 might prove to be helpful for the prevention and treatment of cancer. In particular, we were intrigued  
91 by the well-known anticancer properties of saffron, which is one of the most expensive spices in the

92 world and widely known for its deep yellow colour and exquisite taste. Saffron has long been used  
93 as a medicinal herb to treat several diseases in traditional medicine, and it has found many therapeutic  
94 applications resulting from the plethora of pharmacological properties of its components.<sup>15-18</sup> Saffron  
95 consists of the dried red stigmas of *Crocus sativus* Linnaeus flowers, and its main components can  
96 be grouped in three principle classes: 1) crocins: water-soluble coloured compounds that are  
97 glycosides of the carotenoid crocetin with various sugar ester moieties; 2) picrocrocin: a monoterpene  
98 glycoside that is the main substances responsible for saffron's bitter taste; 3) safranal: the volatile oil  
99 responsible for the characteristic saffron aroma (Figure 2).<sup>19,20</sup>

100 In order to investigate if any of the saffron components possess anti-LDH activity and contribute to  
101 its reported anticancer activity,<sup>16</sup> we started our study by analysing the effects of this spice on the  
102 isolated enzyme. Furthermore, among the main components of saffron, it is widely documented that  
103 both crocin, the crocetin digentiobiose ester, which represents the most important glycoside  
104 carotenoid,<sup>21-24</sup> and also the carotenoid aglycon itself, crocetin, exert anticancer and chemopreventive  
105 effects on several types of cancer cells, and some *in vivo* animal models.<sup>25-29</sup> It is important to note  
106 that the average content of crocin, which behaves as a direct bioprecursor of crocetin when  
107 administered *in vivo*,<sup>30</sup> is about 40 mg/g of stigmas, depending on the geographical location of the  
108 saffron source.<sup>31</sup> Furthermore, the bioavailability of crocetin after oral administration to human  
109 volunteers proved to be highly satisfactory. It was rapidly absorbed and reached maximal plasma  
110 concentration of up to 1  $\mu\text{M}$  after 4-5 hours even at the relatively low dose of 22.5 mg.<sup>32</sup>

111 Interestingly, Kim *et al.* recently reported the effects of crocetin and crocin in several cancer cell  
112 lines. Crocetin induced cell death at submillimolar concentrations ( $\text{IC}_{50}$  values ranging from 0.16 to  
113 0.61 mM in a panel of cancer cells). However, crocin proved to be more potent in the cytotoxicity  
114 assays ( $\text{IC}_{50}$  values ranging from 2.87 to 5.48  $\mu\text{M}$ ). Both expression and activity of *h*LDH-5 were  
115 reduced after treatment of HeLa cells with crocetin and crocin: even in this case, crocetin was more  
116 potent than crocin, since crocetin at 1 mM reduced *h*LDH-5 activity by 34.2 % compared to control  
117 and crocin reached only a 10.5% inhibition at 4 mM. However, these cell-based experiments did not

118 determine whether crocetin or crocin directly interact with *h*LDH-5 because various mechanisms  
119 could be implicated at the cellular level.<sup>33</sup> It could be predicted that the long carbon chains of these  
120 derivatives, characterized by polar moieties (carboxylic groups or sugar portions) at both the  
121 extremities, are well tolerated in the LDH active site. These preliminary results encouraged us to carry  
122 on further detailed studies in order to clarify the specific effects of crocetin and crocin on *h*LDH-5  
123 and in cancer cells, as described below.

124

## 125 **MATERIALS AND METHODS**

126 **Chemicals.** General Procedures and Materials. All solvents and chemicals were used as purchased  
127 without further purification (Aldrich, Alfa Aesar, TCI Europe). The following chemicals were used  
128 for the synthesis of the final compounds and were obtained from commercial suppliers: *trans*-2-  
129 methyl-2-butenic acid, methanol, sulfuric acid, diethyl ether, chloroform, *N*-bromosuccinimide,  
130 benzoylperoxide (70 %, remainder water), fumaraldehyde mono(dimethylacetal),  
131 (carbethoxyethylidene)triphenylphosphorane, triphenylphosphine, activated manganese dioxide,  
132 acetone, 1 M diisobutylaluminum hydride solution in anhydrous hexane, Amberlyst® 15 hydrogen  
133 form, Celite® Hyflo, ethyl acetate, hexane, dichloromethane (DCM), toluene, acetonitrile,  
134 phosphoric acid, sodium hydroxide, sodium sulphate anhydrous, potassium carbonate.  
135 Chromatographic separations were performed on silica gel columns by flash chromatography  
136 (Kieselgel 40, 0.040–0.063 mm; Merck). Reactions were followed by thin layer chromatography  
137 (TLC) on Merck aluminum silica gel (60 F254) sheets that were visualized under a UV lamp.  
138 Evaporation was performed in vacuo (rotating evaporator). Sodium sulfate was always used as the  
139 drying agent. Proton (<sup>1</sup>H) and carbon (<sup>13</sup>C) NMR spectra were obtained with a Bruker Avance III 400  
140 MHz spectrometer using the indicated deuterated solvents. Chemical shifts are given in parts per  
141 million (ppm) ( $\delta$  relative to residual solvent peak for <sup>1</sup>H and <sup>13</sup>C). <sup>1</sup>H-NMR spectra are reported in  
142 this order: multiplicity and number of protons. Standard abbreviation indicating the multiplicity were

143 used as follows: s = singlet, d = doublet, dd = doublet of doublets, ddd = doublet of doublet of  
144 doublets, t = triplet, q = quartet, dq = doublet of quartets, tq = triplet of quartets, qq = quartet of  
145 quartets, quint = quintet, m = multiplet, bq = broad quartet and bd = broad doublet.

146 (*E*)-Methyl 2-methylbut-2-enoate (**2**). *Trans*-2-methyl-2-butenic acid **1** (5.0 g; 50 mmol) was  
147 dissolved in MeOH (50 mL) in a sealed vial, concentrated H<sub>2</sub>SO<sub>4</sub> (0.27 mL) was added dropwise and  
148 the resulting solution was heated at 90 °C for 24 h. The reaction mixture was cooled to room  
149 temperature and concentrated under reduced pressure. The resulting mixture was diluted with Et<sub>2</sub>O,  
150 and then washed successively with a saturated solution of sodium bicarbonate and brine. The organic  
151 phase was dried and evaporated under reduced pressure. The crude methyl tiglate **2** was obtained as  
152 a light yellow oil (34.1 mmol, yield 63%) and was used in the next step without further purification.  
153 <sup>1</sup>H NMR (CDCl<sub>3</sub>) δ (ppm): 1.79 (dq, 3H, *J* = 7.1, 1.2 Hz), 1.83 (quint, 3H, *J* = 1.2 Hz), 3.73 (s, 3H),  
154 6.86 (qq, 1H, *J* = 7.1, 1.4 Hz).

155 (*E*)-Methyl 4-bromo-2-methylbut-2-enoate (**3**) and (*Z*)-methyl 2-(bromomethyl)but-2-enoate (**4**).  
156 Compound **2** (2.0 g; 18 mmol) was dissolved in CHCl<sub>3</sub> (23.0 mL), then NBS (18 mmol) and 70%  
157 BPO (0.7 mmol) were added and the reaction was heated at reflux for 2 h. After cooling to room  
158 temperature, the mixture was concentrated under reduced pressure. Hexane was added to the residue  
159 and the resulting suspension was cooled in an ice bath to promote the precipitation of succinimide,  
160 which was suction filtered off. The filtrate was evaporated. The residue was diluted with AcOEt and  
161 washed with brine. The organic phase was dried and evaporated under vacuum. Mixture of  $\gamma$  and  $\alpha$ -  
162 bromo derivatives was obtained as an orange oil (3.08 g). <sup>1</sup>H NMR (CDCl<sub>3</sub>) δ (ppm, assigned only  
163 significant protons): 3.77 (s, COOMe  $\gamma$  isomer), 3.80 (s, COOMe  $\alpha$  isomer), 4.03 (dq, *J* = 8.5, 0.5  
164 Hz, CH<sub>2</sub>  $\gamma$  isomer), 4.24 (s, CH<sub>2</sub>  $\alpha$  isomer), 6.93 (tq, *J* = 8.5, 1.5 Hz, vinylic proton  $\gamma$  isomer), 7.08 (q,  
165 *J* = 7.3 Hz, vinylic proton  $\alpha$  isomer). Proton integration of these signals suggested the following  
166 composition: 68 %  $\gamma$  isomer, 32 %  $\alpha$  isomer.

167 (*E*)-(4-Methoxy-3-methyl-4-oxobut-2-en-1-yl)triphenylphosphonium bromide (**5**). Mixture of **3** and  
168 **4** (3.08 g) dissolved in toluene (13.7 mL) was treated dropwise with a freshly prepared solution of

169 triphenylphosphine (21.6 mmol) in toluene (21.0 mL) and the reaction mixture, which became  
170 immediately cloudy, was stirred vigorously overnight. A white crystalline solid and a yellow gummy  
171 solid adherent to the walls of the flask formed: the white crystalline solid was suction filtered, washed  
172 with hexane and dried under vacuum and the yellow gummy solid was dissolved in MeOH and dried  
173 under vacuum. Both the fractions were purified by recrystallization from CH<sub>3</sub>CN/AcOEt. Compound  
174 **5** (2.08 g, 4.57 mmol) was obtained as a white crystalline solid (yield on two subsequent steps: 26  
175 %). <sup>1</sup>H NMR (CDCl<sub>3</sub>) δ (ppm): 1.67 (d, 3H, *J* = 3.3 Hz), 3.68 (s, 3H), 5.08 (dd, 2H, *J* = 16.3, 8.0 Hz),  
176 6.64 (bq, 1H, *J* = 6.7 Hz), 7.64-7.94 (m, 15H).

177 (*E*)-Methyl 2-methyl-4-(triphenylphosphoranylidene)but-2-enoate (**6**). To a solution of phosphonium  
178 salt **5** (1.06 g, 2.32 mmol) in CH<sub>2</sub>Cl<sub>2</sub> (9.0 mL) was added dropwise aqueous NaOH 0.5 M (4.6 mL)  
179 and the mixture became immediately orange. After stirring for 10 minutes, the mixture was diluted  
180 with water and extracted with CH<sub>2</sub>Cl<sub>2</sub>, the organic layer was washed with brine, dried and  
181 concentrated under reduced pressure. Crude compound **6** (800 mg, 2.14 mmol) was obtained as an  
182 orange oily solid and used in the subsequent steps without further purification (yield 92%). <sup>1</sup>H NMR  
183 (CDCl<sub>3</sub>) δ (ppm, assigned only significant protons): 1.89 (s, 3H, CH<sub>3</sub>), 3.58 (s, 3H, COOMe).

184 (*2E,4E*)-Ethyl 2-methyl-6-oxohexa-2,4-dienoate (**9**). A solution of fumaraldehyde  
185 mono(dimethylacetal) **8** (300 mg; 0.29 mL, 2.31 mmol) in CH<sub>2</sub>Cl<sub>2</sub> (3.6 mL) was added dropwise to  
186 a solution of (carbethoxyethylidene)triphenylphosphorane **7** (1.09 g; 3.00 mmol) in CH<sub>2</sub>Cl<sub>2</sub> (8.9 mL).  
187 The reaction was stirred at RT overnight. Solvent was reduced under reduced pressure and then the  
188 residue was cooled in an ice bath to promote the precipitation of triphenylphosphine oxide, that was  
189 suction filtered off and washed with petroleum ether. The filtrate was concentrated, affording the  
190 dimethylacetal product in mixture with the corresponding aldehyde derivative, as a white solid (560  
191 mg). The mixture was directly subjected to the next step without further purification. The residue was  
192 dissolved in acetone (9.6 mL), then distilled water (0.15 mL) and Amberlyst 15 (prewashed with  
193 acetone, 102 mg) were added and the reaction was stirred for 1 h. After filtration to remove the resin,  
194 the filtrate was concentrated and purified by flash chromatography over silica gel (*n*-hexane/Et<sub>2</sub>O



195 85:15). Compound **9** was obtained as a yellow oil (355 mg, 2.11 mmol, yield was calculated on two  
196 subsequent steps: 91%). <sup>1</sup>H NMR (CDCl<sub>3</sub>) δ (ppm): 1.33 (t, 3H, *J* = 7.1 Hz), 2.12 (d, 3H, *J* = 1.4 Hz),  
197 4.27 (q, 2H, *J* = 7.1 Hz), 6.39 (dd, 1H, *J* = 15.0, 7.8 Hz), 7.33 (dq, 1H, *J* = 11.8, 1.3 Hz), 7.42 (dd,  
198 1H, *J* = 14.9, 11.8 Hz), 9.70 (d, 1H, *J* = 7.6 Hz).

199 (2*E*,4*E*,6*E*)-Diethyl 2,7-dimethylocta-2,4,6-trienedioate (**10**). Compound **9** (350 mg, 2.08 mmol) was  
200 dissolved in DCM (15.4 mL) and (carbethoxyethylidene)triphenylphosphorane **7** (2.72 mmol) was  
201 added. The reaction was stirred at room temperature for 2 h. The mixture was filtered through a  
202 Büchner funnel partially filled with silica gel and washed with AcOEt. The filtrate was purified by  
203 flash chromatography over silica gel (*n*-hexane/AcOEt 95:5). Compound **10** was obtained as a pearl-  
204 white solid (342 mg, 1.36 mmol, yield 65%). <sup>1</sup>H NMR (CDCl<sub>3</sub>) δ (ppm): 1.32 (t, 6H, *J* = 7.1 Hz),  
205 2.01 (d, 6H, *J* = 1.2 Hz), 4.23 (q, 4H, *J* = 7.1 Hz), 6.80 (dd, 2H, *J* = 7.8, 3.1 Hz), 7.28 (dq, 2H, *J* =  
206 7.9, 1.4 Hz).

207 (2*E*,4*E*,6*E*)-2,7-Dimethylocta-2,4,6-triene-1,8-diol (**11**). Compound **10** (340 mg, 1.35 mmol) was  
208 dissolved in anhydrous hexane (10.4 mL) under Argon atmosphere, cooled to -78 °C and treated  
209 dropwise with a solution 1 M of DIBAL-H in anhydrous hexane (5.3 mL, 5.26 mmol). The resulting  
210 solution was stirred at the same temperature for 5 min and warmed slowly till -20 °C over 3 h. The  
211 reaction was monitored by TLC, showing that the diester was completely reacted. The reaction  
212 mixture was cooled to 0 °C and distilled water (0.3 mL) and silica gel (900 mg) were added. After 45  
213 minutes, K<sub>2</sub>CO<sub>3</sub> (322 mg) and Na<sub>2</sub>SO<sub>4</sub> (488 mg) were added. After 30 minutes, the solids were suction  
214 filtered off and rinsed with CH<sub>2</sub>Cl<sub>2</sub> and AcOEt, the filtrate was concentrated to obtain compound **11**  
215 as a light-yellow solid (214 mg, 1.27 mmol, yield 94%) that was used in the next step without further  
216 purification. <sup>1</sup>H NMR (CDCl<sub>3</sub>) δ (ppm): 1.82 (s, 6H), 4.11 (s, 4H), 6.16 (dq, 2H, *J* = 7.5, 1.4 Hz),  
217 6.45 (dd, 2H, *J* = 7.3, 3.1 Hz).

218 (2*E*,4*E*,6*E*)-2,7-Dimethylocta-2,4,6-trienedial (**12**). Compound **11** (214 mg, 1.27 mmol) was  
219 dissolved in acetone (11.5 mL) and the solution was cooled to 0 °C. Activated MnO<sub>2</sub> (3.32 g, 38.2  
220 mmol) was added and the reaction was stirred overnight at room temperature. The mixture was

221 filtered in a Büchner funnel filled with celite Hyflo® and washed with acetone. The filtrate was  
222 concentrated under reduced pressure and purified by flash chromatography over silica gel (*n*-  
223 hexane/AcOEt 85:15). Compound **12** (152 mg, 0.927 mmol) was obtained as a bright yellow solid  
224 (yield 73%). <sup>1</sup>H NMR (CDCl<sub>3</sub>) δ (ppm): 1.95 (d, 6H, *J* = 1.2 Hz), 6.97-7.13 (m, 4H), 9.55 (s, 2H).  
225 (*2E,4E,6E,8E,10E,12E,14E*)-Dimethyl-2,6,11,15-tetramethylhexadeca-2,4,6,8,10,12,14-  
226 heptaenedioate (**13**). A solution of compound **6** (1.83 mmol) in toluene (3.5 mL) was added to  
227 compound **12** (50.0 mg, 0.305 mmol) in toluene (1.0 mL) and the reaction was heated at 130 °C for  
228 6 h. Then, the mixture was cooled to room temperature and left under stirring overnight. Compound  
229 **13** precipitated as a red brick solid, which was collected by filtration and washed with cold MeOH.  
230 The filtrate was concentrated under reduced pressure, the residue was taken up in 5 mL of MeOH and  
231 heated at 90°C for 30 minutes. The mixture was cooled to room temperature and a second fraction of  
232 pure compound **13** was collected. The total amount of pure compound **13** obtained was 61.4 mg  
233 (0.172 mmol, yield 56%). <sup>1</sup>H NMR (CDCl<sub>3</sub>) δ (ppm): 1.99 (s, 6H), 2.00 (d, 6H, *J* = 1.0 Hz), 3.77 (s,  
234 6H), 6.34-6.40 (m, 2H), 6.55 (dd, 2H, *J* = 15.2, 10.4 Hz), 6.62 (d, 2H, *J* = 14.8 Hz), 6.71 (dd, 2H, *J*  
235 = 7.9, 2.9 Hz), 7.29 (dd, 2H, *J* = 10.7, 1.3 Hz). <sup>13</sup>C NMR (CDCl<sub>3</sub>) δ (ppm): 12.94 (2C), 13.04 (2C),  
236 51.95 (2C), 123.97 (2C), 126.62 (2C), 131.48 (2C), 135.16 (2C), 136.87 (2C), 139.04 (2C), 143.90  
237 (2C), 169.09 (2C).

238 Sodium (*2E,4E,6E,8E,10E,12E,14E*)-2,6,11,15-tetramethylhexadeca-2,4,6,8,10,12,14-  
239 heptaenedioate (**14**) and (*2E,4E,6E,8E,10E,12E,14E*)-2,6,11,15-tetramethylhexadeca-  
240 2,4,6,8,10,12,14-heptaenedioic acid (**15**). Diester **13** (25.0 mg, 0.0701 mmol) was suspended in  
241 MeOH (0.5 mL) and 40 % w/v NaOH (0.7 mL, 7.01 mmol) was added dropwise. The mixture was  
242 heated at reflux overnight. After consumption of the starting material, the mixture was cooled to room  
243 temperature and then to 0 °C and an orange precipitated formed. The solid was collected by filtration,  
244 washing it with cold water and cold MeOH, affording 21.9 mg (0.588 mmol) of the disodium salt **14**  
245 as a bright orange solid (yield 84 %). In order to obtain the diacid **15**, the work-up was accomplished  
246 by evaporating the solvent of the reaction, then the residue was diluted with water and the aqueous

247 phase was washed with Et<sub>2</sub>O. The aqueous layer was acidified with 10 % H<sub>3</sub>PO<sub>4</sub>, to obtain the  
248 precipitation of a red solid that was collected and washed with water and CH<sub>2</sub>Cl<sub>2</sub> (yield 68 %). For  
249 disodium salt **14** <sup>1</sup>H NMR (D<sub>2</sub>O) δ (ppm): 1.95 (s, 6H), 2.00 (s, 6H), 6.43-6.48 (m, 2H), 6.65-6.70  
250 (m, 4H), 6.85 (dd, 2H, *J* = 7.9, 2.9 Hz), 6.97-7.02 (m, 2H). <sup>13</sup>C NMR (D<sub>2</sub>O) δ (ppm): 11.92 (2C),  
251 13.42 (2C), 124.86 (2C), 131.13 (2C), 133.37 (2C), 133.96 (2C), 134.85 (2C), 137.31 (2C), 141.46  
252 (2C), 177.94 (2C). For diacid **15** <sup>1</sup>H NMR (DMSO-*d*<sub>6</sub>) δ (ppm): 1.91 (s, 6H), 1.97 (s, 6H), 6.43-6.53  
253 (m, 2H), 6.61 (dd, 2H, *J* = 14.8, 11.6 Hz), 6.72 (d, 2H, *J* = 15.2 Hz), 6.78-6.88 (m, 2H), 7.20 (bd, 2H,  
254 *J* = 10.8 Hz).

255 **Enzyme assays.** The compounds were evaluated in enzymatic assays to assess their inhibitory  
256 properties against two commercially available purified human isoforms of lactate dehydrogenase,  
257 *h*LDH-5 (tetrameric isoform composed of four A subunits, LDH-A<sub>4</sub>, from human liver, Lee  
258 BioSolutions – USA) and *h*LDH-1 (tetrameric isoform composed of four B subunits, LDH-B<sub>4</sub>, from  
259 human erythrocytes, Lee BioSolutions – USA), as suspensions in 3.1 M ammonium sulfate solution,  
260 with tris chloride, DTT and EDTA, pH 8.3 Dried flower stigmas (saffron pistils) and crocin were  
261 purchased from Sigma-Aldrich. The reaction of lactate dehydrogenase was conducted using the  
262 “forward” direction (pyruvate → lactate) by using an emission wavelength at 460 nm and an  
263 excitation wavelength at 340 nm to monitor the amount of NADH consumed. These assays were  
264 conducted in wells containing 200 μL of a solution comprising the reagents dissolved in 100 mM  
265 phosphate buffer at pH 7.4. DMSO stock solutions of compounds were prepared (the concentration  
266 of DMSO did not exceed 4% during the measurements). Assays were performed in the presence of  
267 40 μM NADH and 200 μM pyruvate, combined with 0.66 ng or 0.38 mU of enzyme in a final volume  
268 of 200 μl (one unit of the enzyme reduces 1 μmol of pyruvate to L-lactate at 37 °C and pH 8.55).  
269 Seven different concentrations (in duplicate for each concentration) of the compound were used to  
270 generate a concentration–response curve. Compound solutions were dispensed in 96-well plates (8  
271 μL), and then the substrate and the cofactor dissolved in the buffer (152 μL) and the enzyme solution  
272 (40 μL) were added. Any possible background fluorescence of the tested compounds, or their

273 quenching of NADH fluorescence, was subtracted. In addition to the compound test wells, each plate  
274 contained maximum and minimum controls. Assay plates were incubated for 15 min, and the final  
275 measurements were performed using a Victor X3 Microplates Reader (PerkinElmer®). IC50 values  
276 were generated using the curve-fitting tool of GraphPad Prism software (GraphPad – USA). In the  
277 enzyme kinetic experiments, the same procedure previously reported by us was followed.<sup>13</sup> The  
278 compound was tested in the presence of scalar NADH or pyruvate concentrations in the NADH or  
279 pyruvate-competition experiments, respectively. In the NADH-competition experiments, the  
280 compound was added (concentration range = 15-45  $\mu\text{M}$ ) to a reaction mixture containing 1.4 mM  
281 pyruvate, scalar concentrations of NADH (concentration range = 10–150  $\mu\text{M}$ ) and 100 mM phosphate  
282 buffer (pH = 7.4). Conversely, in the pyruvate-competition experiments, the reaction mixture  
283 contained 150  $\mu\text{M}$  NADH and scalar concentrations of pyruvate (concentration range = 40–500  $\mu\text{M}$ ).  
284 Finally, LDH solution was added (0.015 U/mL) and the enzyme activity was measured by evaluating  
285 the NADH fluorescence decrease using a Victor X3 Microplates Reader. The experimental data were  
286 analysed with a non-linear regression analysis, using a second order polynomial regression analysis,  
287 and by applying the mixed-model inhibition fit.

288 **Cell lines and cell culture.** A549 cell lines were obtained from ATCC and grown in RPMI 1640  
289 medium with 10 % fetal bovine serum, 100 U/mL penicillin, and 100  $\mu\text{g}/\text{mL}$  streptomycin. HeLa cell  
290 lines were obtained from ATCC and grown in EMEM with 10 % fetal bovine serum, 100 U/mL  
291 penicillin, and 100  $\mu\text{g}/\text{mL}$  streptomycin. Cells were cultured at 37 °C in a 5 % CO<sub>2</sub>– 95% air  
292 humidified atmosphere.

293 **Cytotoxicity evaluation.** HeLa and A549 cells were seeded on 96 well plates at the density of  $1 \times$   
294  $10^3$  cells per well. The cells were continuously treated with various concentrations of compound **14**  
295 for 72 h. Then viability was assessed using the sulforhodamine B (SRB) assay. Cells were fixed with  
296 10% trichloroacetic acid at 4 °C for overnight and then stained with 0.057% SRB in 1 % acetic acid  
297 at room temperature for 30 min. The dye was solubilized in 10 mM Tris base (pH 10.5) and absorption  
298 at 510 nm was measured using a SpectraMax Plus 384 (Molecular Devices, Sunnyvale, CA). Percent

299 death was calculated by subtracting background from all wells and setting 0% death to vehicle-treated  
300 controls. All data are averages of at least three independent replicates. MRC5 cells (from ATCC)  
301 were maintained at 37 °C in a humidified atmosphere containing 5% CO<sub>2</sub> accordingly to the supplier.  
302 Normal ( $1.5 \times 10^4$ ) cells were plated in 96-well culture plates. The day after seeding, vehicle or  
303 compound were added at different concentrations to the medium. Cell viability was measured after  
304 96 h according to the supplier (Promega, G7571) with a Tecan F200 instrument. IC<sub>50</sub> values were  
305 calculated from logistical dose response curves. Averages were obtained from three independent  
306 experiments, and error bars are standard deviations (n = 3).

307 **Assessment of lactate production.** HeLa human cervical carcinoma cells were seeded on 96 well  
308 plates at the density of  $2.5 \times 10^3$  cells per well. When cells reached 80-90 % confluence, the cells  
309 were treated with compound or vehicle control in DMEM medium minus phenol red + 10% dialized  
310 FBS + 100 U/mL penicilin + 100 µg/mL streptomycin for 4 h. Triplicate wells were prepared for each  
311 treatment. Following treatment, the cells were fixed with 10 % trichloroacetic acid for the assessment  
312 of cell viability using SRB assay and the media were collected, and 100 µL were added to 10 µL 10  
313 mM chlorophenylalanine (CPA; the internal standard for GC-MS analysis). Samples were  
314 concentrated, derivatized by a 2h incubation with 50 µL MTBSTFA + 1% TBDMCS (Thermo  
315 Scientific, Waltham, MA) in 50 µL acetonitrile at 80 °C, and immediately analyzed using GC-MS  
316 (Agilent 6890N GC/5973 MS, equipped with an Agilent DB-5 capillary column, 30 m x 320 µm x  
317 0.25 µm, model number J&W 123-5032, Agilent Technologies, Santa Clara, CA) and electron impact  
318 ionization source. The initial oven temperature was 120 °C, held for 5 min; then the temperature was  
319 increased at a rate of 10 °C per minute until a temperature of 250 °C was reached. The temperature  
320 was then increased by 40 °C per minute until a final temperature of 310 °C was reached. The total  
321 run time per sample was 24.5 min. Compounds were identified using AMDIS Chromatogram  
322 software (Amdis, freeware available from [amdis.net](http://amdis.net)) and programmed WIST and Niley commercial  
323 libraries. The integration area of lactate in each sample was divided by the integration area of CPA  
324 in the same sample to achieve a lactate/internal standard ratio. The ratios were normalized by % live

325 and averaged for triplicates. The percentage lactate production over vehicle was calculated and all  
326 data are averages of three independent replicates.

327 **Statistical Analysis.** All statistical analysis was performed using an unpaired, two-tailed student's t  
328 test with p values < 0.05 were considered statistically significant. Values are reported as the means  $\pm$   
329 SD of three or more independent experiments.

330 **Docking Calculations.** The crystal structure of the *h*LDH-5 protein (4M49 PDB code<sup>34</sup>), was taken  
331 from the Protein Data Bank.<sup>35</sup> After adding hydrogen atoms, the protein was minimized using  
332 Amber14 software and the ff14SB force field at 300 K (in order to reproduce the room temperature  
333 used in the enzymatic assay).. The complex was placed in a rectangular parallelepiped waterbox, an  
334 explicit solvent model for water, TIP3P, was used and the complex was solvated with a 10 Å water  
335 cap. Sodium ions were added as counterions to neutralize the system. Two steps of minimization were  
336 then carried out; in the first stage, we kept the protein fixed with a position restraint of 500 kcal/molÅ<sup>2</sup>  
337 and we solely minimized the positions of the water molecules. In the second stage, we minimized the  
338 entire system through 5000 steps of steepest descent followed by conjugate gradient (CG) until a  
339 convergence of 0.05 kcal/Åmol. The ligands were built using Maestro and were minimized by means  
340 of Macromodel in a water environment using the CG method until a convergence value of 0.05  
341 kcal/Åmol, using the MMFFs force field and a distance-dependent dielectric constant of 1.0.  
342 AUTODOCK Tools,<sup>36</sup> was used to define the torsion angles in the ligands, to add the solvent model  
343 and to assign partial atomic charges to the ligand and the protein. The docking site used for  
344 AUTODOCK calculations was defined in such a manner that it was constituted by all residues within  
345 10 Å of the reference ligand and NADH co-factor in the X-ray crystal structure. The energetic maps  
346 were calculated using a grid spacing of 0.375 Å and a distance dependent function of the dielectric  
347 constant. The ligand was subjected to 200 docking runs of the AUTODOCK search using the  
348 Lamarckian genetic algorithm (LGA) and employing 10 000 000 energy evaluations; the number of  
349 individuals in the initial population was set to 500 and a maximum of 10 000 000 generations were

350 simulated during the docking run; an rms tolerance of 2.0 Å was used to carry out the cluster analysis  
351 of the docking solutions and all the other settings were left as their defaults.

352 **MD simulations.** All simulations were performed using AMBER, version 14.<sup>37</sup> MD simulations were  
353 carried out using the ff14SB force field at 300 K. The complex was placed in a rectangular  
354 parallelepiped water box. An explicit solvent model for water, TIP3P, was used, and the complexes  
355 were solvated with a 20 Å water cap. Chlorine ions were added as counterions to neutralize the  
356 system. Prior to MD simulations, two steps of minimization were carried out using the same  
357 procedure described above. Particle mesh Ewald (PME) electrostatics and periodic boundary  
358 conditions were used in the simulation.<sup>38</sup> The MD trajectory was run using the minimized structure  
359 as the starting conformation. The time step of the simulations was 2.0 fs with a cutoff of 10 Å for the  
360 nonbonded interaction, and SHAKE was employed to keep all bonds involving hydrogen atoms rigid.  
361 Constant-volume periodic boundary MD was carried out for 0.5 ns, during which the temperature  
362 was raised from 0 to 300 K. Then 19.5 ns of constant pressure periodic boundary MD was carried out  
363 at 300 K using the Langevin thermostat to maintain constant the temperature of our system. All the  $\alpha$   
364 carbons of the protein were blocked with a harmonic force constant of 10 kcal/mol•Å<sup>2</sup> for the first  
365 3.5 ns. General Amber force field (GAFF) parameters were assigned to the ligand, while partial  
366 charges were calculated using the AM1-BCC method as implemented in the Antechamber suite of  
367 AMBER 14. The final structures of the complexes were obtained as the average of the last 16.5 ns of  
368 MD minimized by the CG method until a convergence of 0.05 kcal/mol•Å<sup>2</sup>. The average structures  
369 were obtained using the Cpptraj program<sup>39</sup> implemented in AMBER 14.

370 **Binding Energy Evaluation.** The evaluation of the binding energy associated to the different ligand-  
371 protein complexes analyzed through MD simulations was carried out using AMBER 14. The  
372 trajectories relative to the last 16.5 ns of each simulation were extracted and used for the calculation,  
373 for a total of 165 snapshots (at time intervals of 100 ps). Van der Waals, electrostatic and internal  
374 interactions were calculated with the SANDER module of AMBER 14, whereas polar energies were  
375 calculated using both the Generalized Born and the Poisson–Boltzman methods with the MM-PBSA

376 module of AMBER 14. Dielectric constants of 1 and 80 were used to represent the gas and water  
377 phases, respectively, while the MOLSURF program was employed to estimate the nonpolar energies.  
378 The entropic term was considered as approximately constant in the comparison of the ligand–protein  
379 energetic interactions.

380

## 381 **RESULTS AND DISCUSSION**

### 382 **LDH inhibition assays of saffron polar extract**

383 Commercially available red stigmatic lobes of saffron were dissolved in a suitable polar solvent, such  
384 as dimethyl sulfoxide (DMSO), and the polar saffron chemical constituents were extracted, which we  
385 hypothesized would have a higher chance to efficiently interact with the highly hydrophilic catalytic  
386 site of *h*LDH-5 than non-polar components. The saffron DMSO extract was then serially diluted and  
387 tested on *h*LDH-5 and *h*LDH-1 purified isoforms to determine its inhibition potency. At the maximum  
388 tested concentration of 0.8 mg/mL, we observed an inhibition of 52% of the activity of *h*LDH-5  
389 (corresponding to an IC<sub>50</sub> value of 0.653 mg/mL) and of 49% of the activity of *h*LDH-1 (resulting in  
390 an IC<sub>50</sub> value of 0.717 mg/mL) by the saffron solution. The noticeable activity of the crude saffron  
391 polar extract served as the starting point for the investigation into this dietary natural product and  
392 the identification of the constituents responsible for the inhibition of LDH enzymes.

393

### 394 **Chemical synthesis of crocetin**

395 Unlike crocin, which is commercially available at a reasonable level of purity, it was not possible to  
396 easily purchase or extract crocetin in sufficient purity and amount to complete further biological  
397 studies. Therefore, crocetin was synthesized by a multi-step synthesis. Crocetin possesses a diterpenic  
398 and symmetrical structure, possessing alternating *trans* double bonds in the alkyl chain, four methyl  
399 groups and carboxylic groups at both ends of the backbone. The synthesis of this carotenoid required  
400 the formation of two fragments that converged in the last steps: 1) synthesis of the central dialdehyde



401 unsaturated carbon chain (compound **12**, Scheme 1, part B) and 2) formation of a  
402 triphenylphosphoranylide intermediate (compound **6**, Scheme 1, part A), which would be condensed  
403 at both the terminal parts of the previous chain.<sup>40</sup> The first part of this synthetic pattern was the  
404 preparation of (*E*)-methyl 2-methyl-4-(triphenylphosphoranylidene)but-2-enoate **6**, which was  
405 condensed with dialdehyde **12** to obtain dimethyl crocetinate **13**, an immediate precursor of crocetin  
406 (Scheme 1). Initially, a methanolic solution of *trans*-2-methyl-2-butenic acid **1**, also called tiglic  
407 acid, was heated in the presence of H<sub>2</sub>SO<sub>4</sub> to obtain the methyl tiglate **2** (Scheme 1). Methyl tiglate is  
408 a highly volatile compound, so it was necessary to take some precautions: *a*) the reaction was  
409 performed in a sealed vial in order to minimize the evaporation of the product during heating, and *b*)  
410 the workup procedure avoided exposing this intermediate to a high vacuum. The product was obtained  
411 as a crude light yellow oil that was subsequently used in the next step without further purification.  
412 Methyl ester **2** was subjected to a radical bromination with *N*-bromosuccinimide (NBS) in the  
413 presence of the radical initiator benzoyl peroxide (BPO), which afforded a mixture of the two possible  
414 regioisomers,  $\gamma$  and  $\alpha$  allylic bromides (compounds **3** and **4**, respectively). The relative amounts of  
415 the two regioisomers were evaluated by <sup>1</sup>H-NMR (signals of methylene protons, see experimental  
416 section) and  $\gamma$  and  $\alpha$  bromides were present in a 3:2 ratio, respectively. The mixture was used in the  
417 next step without further purification. The mixture of compounds **3** and **4** was dissolved in toluene  
418 and combined with a slight excess of triphenylphosphine to get phosphonium salts. At this time, the  
419 triphenylphosphonium salt of methyl  $\gamma$ -bromotiglate **5** was isolated as a pure regioisomer by  
420 recrystallization from CH<sub>3</sub>CN/AcOEt (Scheme 1). Compound **5** was treated with aqueous sodium  
421 hydroxide to afford compound **6**. However the formed triphenylphosphoranylide proved to be  
422 particularly instable upon exposure to atmospheric oxygen. These observations led us to perform the  
423 reaction under an Argon atmosphere and avoid purification of this compound. The reaction was  
424 monitored via the presence of representative signals in the <sup>1</sup>H-NMR spectrum (see experimental  
425 section) and compound **6** was prepared immediately before its use in the subsequent Wittig reaction  
426 (Scheme 1).

427 The second fragment of the synthesis involved the preparation of dialdehyde **12** (Scheme 1), which  
428 was to be condensed with phosphoranylide **6**. The synthesis of **12** commenced with a Wittig reaction  
429 between commercially available fumaraldehyde mono(dimethyl acetal) **8** and  
430 (carbethoxyethylidene)triphenylphosphorane **7**, providing a mixture of both the desired condensation  
431 product still possessing the dimethyl acetal portion (structure not shown) and condensation product **9**  
432 possessing the free aldehyde moiety. This resulted the acetal group being partially removed under  
433 these reaction conditions. Considering that the next step of the synthesis involved the deprotection of  
434 the acetal moiety to obtain aldehyde **9**, the mixture was treated with amberlyst 15 in a biphasic solvent  
435 system consisting of water and acetone, which lead to the complete hydrolysis of the dimethyl acetal  
436 group to afford pure aldehyde **9**. Amberlyst 15 was used as an acid catalyst due to its not affecting  
437 the highly reactive double bonds present in the structure of the starting material and its ease of  
438 purification. A second Wittig reaction with (carbethoxyethylidene)triphenylphosphorane **7** gave the  
439 symmetric diester intermediate **10**. Compound **10** was then reduced to form the corresponding  
440 dialcohol **11** via an excess of diisobutylaluminum hydride (DIBAL-H) and anhydrous hexane as  
441 solvent. The subsequent partial oxidation of the allylic alcoholic groups of compound **11** was  
442 performed with MnO<sub>2</sub> to give the corresponding dialdehyde **12**. Compound **12** was subjected to a  
443 double Wittig reaction with the triphenylphosphoranylide **6**, thus extending the unsaturated carbon  
444 chain at both terminals. The resulting dimethyl ester of crocetin **13** precipitated as a red powder and  
445 was isolated by filtration. The precipitate was recrystallized from MeOH to obtaine material of  
446 sufficient purity. Compound **13** was saponified with aqueous NaOH to give the corresponding sodium  
447 salt (disodium crocetinate **14**), which precipitated as a bright orange solid (step g, Scheme 1).  
448 Alternatively, the saponification was followed by acidification with phosphoric acid to obtain the free  
449 diacid crocetin **15** (step h, Scheme 1).<sup>41</sup>

450

451 **LDH inhibition assays of crocetin and crocin**

452 Synthetic dibasic crocetin (compound **14**), its dimethyl ester precursor **13**, and commercially  
453 available crocin **16** were tested on *h*LDH-5 and *h*LDH-1 purified isoforms to determine their  
454 inhibitory properties, relative to galloflavin, which served as a positive control (Table 1).<sup>12</sup> The  
455 disodium salt **14** was preferred to free acid **15** in these biological assays, since the salt form readily  
456 dissolved in the aqueous buffer without any additional organic solvent. Nevertheless, crocetin as  
457 diacid (**15**) was tested to confirm the inhibitory activity on the enzyme. Compound **13** was found to  
458 be completely inactive, displaying  $IC_{50}$  values greater than 200  $\mu$ M for both isoforms. Conversely,  
459 disodium salt **14**, showed noticeable inhibition of *h*LDH-5 ( $IC_{50} = 54.9 \mu$ M) and it was selective for  
460 this isoform, proving to be less active on isoform 1 ( $IC_{50} > 200 \mu$ M). The  $IC_{50}$  value of diacid **15**  
461 nicely overlaps with that of its disodium salt (Table 1). Reference inhibitor galloflavin was 1.7-fold  
462 less potent than compound **14**, and it also inhibited isoform 1 of the enzyme with a similar potency.  
463 Crocin **16** was less effective in the inhibition of *h*LDH-5 relative to crocetin, with an  $IC_{50}$  value  
464 similar to that of galloflavin ( $IC_{50} = 95.7 \mu$ M), and it showed selectivity towards isoform 1 ( $IC_{50} =$   
465  $59.8 \mu$ M). In order to complete the biochemical characterization of crocetin, a kinetic assay was  
466 performed by applying a mixed-model inhibition fit to the second order polynomial regression  
467 analysis of the rate of conversion of NADH to  $NAD^+$  to obtain  $K_i$  values in the NADH-competition  
468 experiments. In these experiments we measured an apparent Michaelis–Menten constant ( $K_M$ ) of 20  
469  $\mu$ M and a  $K_i$  value of 25.6  $\mu$ M, which is consistent with the  $IC_{50}$  values of both forms of crocetin  
470 (disodium salt **14** and diacid **15**) reported in Table 1. Similarly, in the pyruvate-competition  
471 experiments in which the  $K_M$  value was of 100  $\mu$ M, the resulting  $K_i$  value was of 21.1  $\mu$ M.  
472 From a structural point of view, we can conclude that the replacement of the two carboxylic acids of  
473 crocetin by methyl ester groups, as in compound **13**, or the esterification with sugar moieties, as in  
474 crocin **16**, led to a loss of inhibitory activity (in the case of **13**) or a slight decrease in activity and a  
475 marked loss of selectivity for isoform 5 (in the case of **16**), thus identifying crocetin as the most active  
476 compound among these saffron derivatives.

477

478 **Inhibition of cancer cell proliferation and reduction of cellular lactate production**

479 Following the results previously obtained with isolated LDH enzyme isoforms, studies in cancer cells  
480 were focused on the disodium salt of crocetin **14** because it was found to be the most active *h*LDH-5  
481 inhibitor among the saffron derivatives herein studied. Compound **14** was evaluated for growth  
482 inhibitory effects on two different cancer cell lines, HeLa (human cervical carcinoma cells) and A549  
483 (human lung carcinoma cells), after 72 hours of incubation. Cell death was assessed by  
484 Sulforhodamine B (SRB) staining, as previously described<sup>42</sup> and the cytotoxic potency of the tested  
485 compound was expressed as IC<sub>50</sub> values, which represent the concentration of a compound that is  
486 required for the 50% inhibition of cell proliferation. Compound **14** was able to counteract cancer cell  
487 growth both in A549 and in HeLa cells with similar IC<sub>50</sub> values of 114.0 ± 8.0 and 113.0 ± 11.1 μM,  
488 respectively (Figure 3, panel A), which may be considered as respectable values for a food  
489 component. Furthermore, **14** proved to be completely inactive against noncancerous human fibroblast  
490 lung cells (MRC5 IC<sub>50</sub> > 500 μM). After the preliminary biochemical evaluation on the isolated  
491 enzymes and the cytotoxicity assays on two cancer cell lines, this compound was also assayed for its  
492 ability to inhibit the production of lactate in cancer cells. To this end, HeLa cells were treated with  
493 **14** in phosphate buffer saline (PBS) for 6 hours and then the cell culture medium was extracted and  
494 mixed with a known amount of chlorophenylalanine (CPA, internal standard) and dried. Concentrated  
495 samples were reacted with *N*-methyl-*N*-*tert*-butyldimethylsilyltrifluoroacetamide (MTBSTFA) for  
496 derivatization of lactate, which was needed for its GC-MS detection and quantification. The cells  
497 were fixed and biomass was measured using SRB. Crocetin disodium salt **14** was tested at a 100 μM  
498 concentration. As previously reported, the GC-MS analysis of cell culture media for the quantitative  
499 determination of extracellular lactate was preferred over other methods, since it allows a highly  
500 sensitive determination of low micromolar lactate concentrations.<sup>43</sup> As shown in Figure 3 (Panel B),  
501 compound **14** reduced lactate production of about 20 % compared to PBS control at 100 μM after 6  
502 h incubation.

503

## 504 **Molecular modelling studies**

505 To rationalize how compound **14** can interact with the *h*LDH-5 protein, molecular docking studies  
506 followed by molecular dynamic (MD) simulations and binding energy determinations were carried  
507 out. Compound **14** was docked into the crystal structure of the *h*LDH-5 protein (4M49 PDB code)  
508 using AUTODOCK software.<sup>36</sup> The 200 different docking results generated were clustered using a  
509 root-mean square deviation (RMSD) threshold of 2.0 Å and the so obtained 5 clusters of solutions  
510 were considered for further studies (see the Experimental section for details). For each cluster, the  
511 docking pose associated with the best estimated binding energy was selected as a representative  
512 binding mode. The stability of the 5 different binding modes was then assessed through 20 ns of MD  
513 simulation studies with explicit water molecules, as described in the Experimental section. The 5 MD  
514 trajectories obtained in this way were further analyzed through the Molecular Mechanics - Poisson  
515 Boltzmann Surface Area (MM-PBSA) method,<sup>44</sup> which was shown to accurately estimate the ligand-  
516 receptor energy interaction.<sup>45,46</sup> This approach averages the contributions of gas phase energies,  
517 solvation free energies, and solute entropies calculated for snapshots of the complex molecule as well  
518 as the unbound components extracted from MD trajectories, according to the procedure fully  
519 described in the Experimental section. The MM-PBSA results (Table 2) suggest that there is one  
520 docking pose that is the most favorable, as it shows an interaction energy  $\Delta$ PBSA = -29.2 kcal/mol,  
521 more than 8 kcal/mol higher than all the other binding poses (docking pose 1, Table 2).

522 Figure 4 shows the energy minimized average structures of the last 16.5 ns of *h*LDH-5 complexed  
523 with the hypothesized binding pose of compound **14**. The ligand interacts within the pyruvate binding  
524 site and points towards the binding site entrance. One of the two carboxylic groups forms a hydrogen  
525 bond with the catalytic H193, whereas the second carboxylic end forms a strong ionic couple with  
526 positively charged residue K57. Although the binding of the compound to the enzyme active site is  
527 mainly driven by the interactions of the two carboxylic ends, the internal carbon chain of the ligand  
528 also shows lipophilic interactions along the *h*LDH-5 surface and, in particular, with A30, V31, V136  
529 and I252, which represent fundamental additive contributions to the binding process.

530 In conclusion, an investigation into the bioactive properties of saffron extract led to the discovery of  
531 LDH-inhibitory activity, to carotenoid crocetin. Additionally, these compounds mitigated  
532 proliferation of glycolytic cancer cells. In order to unambiguously establish the effective activity of  
533 this natural compound, a multi-step chemical synthesis was implemented for the production of pure  
534 crocetin. Its moderate inhibition potency against the isolated LDH-enzyme, which frankly cannot  
535 compete with several synthetic inhibitors previously described, should not be considered as a limiting  
536 factor since crocetin is part of a spice (saffron) utilized in aliments, whose relative safety has been  
537 now established by millennia of culinary tradition employing it in many recipes. It should be  
538 acknowledged the oral LD<sub>50</sub> for saffron in mice was found to be 20 g/kg, although oral administration  
539 of the saffron extract at concentrations from 0.1 to 5 g/kg was demonstrated to be non-toxic in mice.<sup>47</sup>  
540 Furthermore, a recent study revealed that administration of up to 400 mg / day of saffron for 1 week  
541 to healthy human volunteers did not cause any clinically significant effects,<sup>48</sup> thus confirming its  
542 higher safety when compared to classical anticancer drugs. For these reasons, this study contributes  
543 to appreciate the role of saffron in the prevention and treatment of cancer when utilized in  
544 combination with standard-of-care preventive and therapeutic options.

545

546

547

548

## 549 **ACKNOWLEDGEMENTS**

550 We are grateful to the NIH grants R01-GM098453 (to PJH and FM), the University of Pisa, and the  
551 University of Illinois for support of this work.

552

- 554 1. Warburg, O. On the origin of cancer cells. *Science* **1956**, *123*, 309-314.
- 555 2. Granchi, C.; Minutolo, F. Anticancer agents that counteract tumor glycolysis.
- 556 *ChemMedChem* **2012**, *7*, 1318-1350.
- 557 3. Granchi, C.; Fancelli, D.; Minutolo, F. An update on therapeutic opportunities offered by
- 558 cancer glycolytic metabolism. *Bioorg. Med. Chem. Lett.* **2014**, *24*, 4915-4925.
- 559 4. Kanno, T.; Sudo, K.; Maekawa, M.; Nishimura, Y.; Ukita, M.; Fukutake, K. Lactate
- 560 dehydrogenase M-subunit deficiency: a new type of hereditary exertional myopathy. *Clin.*
- 561 *Chim. Acta* **1989**, *173*, 89-98.
- 562 5. Fantin, V. R.; St-Pierre, J.; Leder, P. Attenuation of LDH-A expression uncovers a link
- 563 between glycolysis, mitochondrial physiology, and tumor maintenance. *Cancer Cell* **2006**,
- 564 *9*, 425-434.
- 565 6. Granchi, C.; Paterni, I.; Rani, R.; Minutolo, F. Small-molecule inhibitors of human LDH5.
- 566 *Future Med. Chem.* **2013**, *5*, 1967-1991.
- 567 7. Gomez, M. S.; Piper, R. C.; Hunsaker, L. A.; Royer, R. E.; Deck, L. M.; Makler, M. T.;
- 568 Vander Jagt, D. L. Substrate and cofactor specificity and selective inhibition of lactate
- 569 dehydrogenase from the malarial parasite *P. falciparum*. *Mol. Biochem. Parasitol.* **1997**, *90*,
- 570 235-246.
- 571 8. Wang, Z.; Wang, D.; Han, S.; Wang, N.; Mo, F.; Loo, T. Y.; Shen, J.; Huang, H.; Chen, J.
- 572 Bioactivity-guided identification and cell signaling technology to delineate the lactate
- 573 dehydrogenase A inhibition effects of *Spatholobus suberectus* on breast cancer. *PLoS One*
- 574 **2013**, *8*, e56631.
- 575 9. Arora, R.; Schmitt, D.; Karanam, B.; Tan, M.; Yates, C.; Dean-Colomb W. Inhibition of the
- 576 Warburg effect with a natural compound reveals a novel measurement for determining the
- 577 metastatic potential of breast cancers. *Oncotarget* **2015**, *6*, 662-678.
- 578 10. Ramanathan, R.; Mancini, R. A.; Suman, S. P.; Beach, C. M. Covalent binding of 4-
- 579 hydroxy-2-nonenal to lactate dehydrogenase decreases NADH formation and metmyoglobin
- 580 reducing activity. *J. Agric. Food Chem.* **2014**, *62*, 2112-2117.
- 581 11. Deiab, S.; Mazzio, E.; Eyunni, S.; McTier, O.; Mateeva, N.; Elshami, F.; Soliman, K. F.
- 582 1,2,3,4,6-Penta-O-galloylglucose within *Galla Chinensis* Inhibits Human LDH-A and
- 583 Attenuates Cell Proliferation in MDA-MB-231 Breast Cancer Cells. *Evid. Based*
- 584 *Complement. Alternat. Med.* **2015**, *2015*, 276946.
- 585 12. Manerba, M.; Vettraino, M.; Fiume, L.; Di Stefano, G.; Sartini, A.; Giacomini, E.;
- 586 Buonfiglio, R.; Roberti, M.; Recanatini, M. Galloflavin (CAS 568-80-9): a novel inhibitor
- 587 of lactate dehydrogenase. *ChemMedChem* **2012**, *7*, 311-317.
- 588 13. Bader, A.; Tuccinardi, T.; Granchi, C.; Martinelli, A.; Macchia, M.; Minutolo, F.; De
- 589 Tommasi, N.; Braca, A. Phenylpropanoids and flavonoids from *Phlomis kurdica* as
- 590 inhibitors of human lactate dehydrogenase. *Phytochemistry* **2015**, *116*, 262-268.
- 591 14. Deiab, S.; Mazzio, E.; Messeha, S.; Mack, N.; Soliman, K. F. High-Throughput Screening
- 592 to Identify Plant Derived Human LDH-A Inhibitors. *Eur. J. Med. Plants* **2013**, *3*, 603-615.
- 593 15. Bathaie, S. Z.; Mousavi, S. Z. New applications and mechanisms of action of saffron and its
- 594 important ingredients. *Crit. Rev. Food Sci. Nutr.* **2010**, *50*, 761-786.
- 595 16. Christodoulou, E.; Kadoglou, N. P.; Kostomitsopoulos, N.; Valsami, G. Saffron: a natural
- 596 product with potential pharmaceutical applications. *J. Pharm. Pharmacol.* **2015**, *67*, 1634-
- 597 1649.
- 598 17. Geromichalos, G. D.; Lamari, F. N.; Papandreou, M. A.; Trafalis, D. T.; Margarity, M.;
- 599 Papageorgiou, A.; Sinakos, Z. Saffron as a source of novel acetylcholinesterase inhibitors:

- 600 molecular docking and in vitro enzymatic studies. *J. Agric. Food. Chem.* **2012**, *60*, 6131-  
601 618.
- 602 18. Ahrazem, O.; Rubio-Moraga, A.; Nebauer, S. G.; Molina, R. V.; Gómez-Gómez, L. Saffron:  
603 Its Phytochemistry, Developmental Processes, and Biotechnological Prospects. *J. Agric.*  
604 *Food Chem.* **2015**, *63*, 8751-8764.
- 605 19. Cossignani, L.; Urbani, E.; Simonetti, M. S.; Maurizi, A.; Chiesi, C.; Blasi, F.  
606 Characterisation of secondary metabolites in saffron from central Italy (Cascia, Umbria).  
607 *Food Chem.* **2014**, *143*, 446-451.
- 608 20. Nescatelli, R.; Carradori, S.; Marini, F.; Caponigro, V.; Bucci, R.; De Monte, C.; Mollica,  
609 A.; Mannina, L.; Ceruso, M.; Supuran, C.T.; Secci, D. Geographical characterization by  
610 MAE-HPLC and NIR methodologies and carbonic anhydrase inhibition of Saffron  
611 components. *Food Chem.* **2017**, *221*, 855-863.
- 612 21. Lu, P.; Lin, H.; Gu, Y.; Li, L.; Guo, H.; Wang, F.; Qiu, X. Antitumor effects of crocin on  
613 human breast cancer cells. *Int. J. Clin. Exp. Med.* **2015**, *8*, 20316-20322.
- 614 22. Chen, S.; Zhao, S.; Wang, X.; Zhang, L.; Jiang, E.; Gu, Y.; Shangguan, A. J.; Zhao, H.; Lv,  
615 T.; Yu, Z. Crocin inhibits cell proliferation and enhances cisplatin and pemetrexed  
616 chemosensitivity in lung cancer cells. *Transl. Lung Cancer Res.* **2015**, *4*, 775-783.
- 617 23. Xia, D. Ovarian cancer HO-8910 cell apoptosis induced by crocin in vitro. *Nat. Prod.*  
618 *Commun.* **2015**, *10*, 249-252.
- 619 24. D'Alessandro, A. M.; Mancini, A.; Lizzi, A. R.; De Simone, A.; Marroccella, C. E.;  
620 Gravina, G. L.; Tatone, C.; Festuccia, C. Crocus sativus stigma extract and its major  
621 constituent crocin possess significant antiproliferative properties against human prostate  
622 cancer. *Nutr. Cancer* **2013**, *65*, 930-942.
- 623 25. Gutheil, W. G.; Reed, G.; Ray, A.; Anant, S.; Dhar, A. Crocetin: an agent derived from  
624 saffron for prevention and therapy for cancer. *Curr. Pharm. Biotechnol.* **2012**, *13*, 173-179.
- 625 26. Li, S.; Jiang, S.; Jiang, W.; Zhou, Y.; Shen, X. Y.; Luo, T.; Kong, L. P.; Wang, H. Q.  
626 Anticancer effects of crocetin in human esophageal squamous cell carcinoma KYSE-150  
627 cells. *Oncol. Lett.* **2015**, *9*, 1254-1260.
- 628 27. Festuccia, C.; Mancini, A.; Gravina, G. L.; Scarsella, L.; Llorens, S.; Alonso, G. L.; Tatone,  
629 C.; Di Cesare, E.; Jannini, E. A.; Lenzi, A.; D'Alessandro, A. M.; Carmona, M. Antitumor  
630 effects of saffron-derived carotenoids in prostate cancer cell models. *BioMed Res. Int.* **2014**,  
631 *2014*, 135048.
- 632 28. He, K.; Si, P.; Wang, H.; Tahir, U.; Chen, K.; Xiao, J.; Duan, X.; Huang, R.; Xiang, G.  
633 Crocetin induces apoptosis of BGC-823 human gastric cancer cells. *Mol. Med. Rep.* **2014**, *9*,  
634 521-526.
- 635 29. Bathaie, S. Z.; Hoshyar, R.; Miri, H.; Sadeghizadeh, M. Anticancer effects of crocetin in  
636 both human adenocarcinoma gastric cancer cells and rat model of gastric cancer. *Biochem.*  
637 *Cell Biol.* **2013**, *91*, 397-403.
- 638 30. Asai, A.; Nakano, T.; Takahashi, M.; Nagao, A. Orally administered crocetin and crocins  
639 are absorbed into blood plasma as crocetin and its glucuronide conjugates in mice. *J. Agr.*  
640 *Food Chem.* **2005**, *53*, 7302-7306.
- 641 31. Caballero-Ortega, H.; Pereda-Miranda, R.; Abdullaev, F. I. HPLC quantification of major  
642 active components from 11 different saffron (*Crocus sativus* L.) sources. *Food Chem.* **2007**,  
643 *100*, 1126-1131.
- 644 32. Umigai, N.; Murakami, K.; Ulit, M.; Antonio, L.; Shirotori, M.; Morikawa, H.; Nakano, T.  
645 The pharmacokinetic profile of crocetin in healthy adult human volunteers after a single oral  
646 administration. *Phytomedicine* **2011**, *18*, 575-578.



- 647 33. Kim, S. H.; Lee, J. M.; Kim, S. C.; Park, C. B.; Lee, P. C. Proposed cytotoxic mechanisms  
648 of the saffron carotenoids crocin and crocetin on cancer cell lines. *Biochem. Cell Biol.* **2014**,  
649 *92*, 105-111.
- 650 34. Fauber, B. P.; Dragovich, P. S.; Chen, J.; Corson, L. B.; Ding, C. Z.; Eigenbrot, C.;  
651 Giannetti, A. M.; Hunsaker, T.; Labadie, S.; Liu, Y.; Malek, S.; Peterson, D.; Pitts, K.;  
652 Sideris, S.; Ultsch, M.; VanderPorten, E.; Wang, J.; Wei, B.; Yen, I.; Yue, Q. Identification  
653 of 2-amino-5-aryl-pyrazines as inhibitors of human lactate dehydrogenase. *Bioorg. Med.*  
654 *Chem. Lett.* **2013**, *23*, 5533-5539.
- 655 35. Berman, H. M.; Westbrook, J.; Feng, Z.; Gilliland, G.; Bhat, T. N.; Weissig, H.; Shindyalov,  
656 I. N.; Bourne, P. E. The Protein Data Bank. *Nucleic Acids Res.* **2000**, *28*, 235-242.
- 657 36. Morris, G. M.; Huey, R.; Lindstrom, W.; Sanner, M. F.; Belew, R. K.;Goodsell, D. S.;  
658 Olson, A. J. AutoDock4 and AutoDockTools4: Automated docking with selective receptor  
659 flexibility. *J. Comput. Chem.* **2009**, *30*, 2785-2791.
- 660 37. Case, D. A.; Berryman, J. T.; Betz, R. M.; Cerutti, D. S.; Cheatham, T. E., III; Darden, T.  
661 A.; Duke, R. E.; Giese, T. J.; Gohlke, H.; Goetz, A. W.; Homeyer, N.; Izadi, S.; Janowski,  
662 P.; Kaus, J.; Kovalenko, A.; Lee, T. S.; LeGrand, S.; Li, P.; Luchko, T.; Luo, R.; Madej, B.;  
663 Merz, K. M.; Monard, G.; Needham, P.; Nguyen, H.; Nguyen, H. T.; Omelyan, I.; Onufriev,  
664 A.; Roe, D. R.; Roitberg, A.; Salomon-Ferrer, R.; Simmerling, C. L.; Smith, W.; Swails, J.;  
665 Walker, R. C.; Wang, J.; Wolf, R. M.; Wu, X.; York, D. M.; Kollman, P. A. AMBER,  
666 version 14; University of California: San Francisco, CA, **2015**.
- 667 38. York, D. M.; Darden, T. A.; Pedersen, L. G. The Effect of Long-Range Electrostatic  
668 Interactions in Simulations of Macromolecular Crystals - a Comparison of the Ewald and  
669 Truncated List Methods. *J. Chem. Phys.* **1993**, *99*, 8345-8348.
- 670 39. Roe, D. R.; Cheatham, T. E., 3rd. PTRAJ and CPPTRAJ: Software for Processing and  
671 Analysis of Molecular Dynamics Trajectory Data. *J. Chem. Theory Comput.* **2013**, *9*, 3084-  
672 3095.
- 673 40. Gainer, J. L.; Grabiak, R. C. Bipolar trans carotenoid salts and their uses. US2014051759,  
674 **2014**.
- 675 41. Van Calsteren, M-R.; Bissonnette, M. C.; Cormier, F.; Dufresne, C.; Ichi, T.; LeBlanc, J. C.  
676 Y.; Perreault, D.; Roewer, I. Spectroscopic Characterization of Crocetin Derivatives from  
677 *Crocus sativus* and *Gardenia jasminoides*. *J. Agric. Food Chem.* **1997**, *45*, 1055-1061.
- 678 42. Vichai, V.; Kirtikara, K. Sulforhodamine B colorimetric assay for cytotoxicity screening.  
679 *Nat. Protoc.* **2006**, *1*, 1112-1116.
- 680 43. a) Granchi, C.; Calvaresi, E. C.; Tuccinardi, T.; Paterni, I.; Macchia, M.; Martinelli, A.,  
681 Hergenrother, P. J.; Minutolo, F. Assessing the differential action on cancer cells of LDH-A  
682 inhibitors based on the N-hydroxyindole-2-carboxylate (NHI) and malonic (Mal) scaffolds.  
683 *Org. Biomol. Chem.* **2013**, *11*, 6588-6596; b) Calvaresi, E. C.; Granchi, C.; Tuccinardi, T.;  
684 Di Bussolo, V.; Huigens, R. W. 3rd.; Lee, H. Y.; Palchaudhuri, R.; Macchia, M.; Martinelli,  
685 A.; Minutolo, F.; Hergenrother, P. J. Dual targeting of the Warburg effect with a glucose-  
686 conjugated lactate dehydrogenase inhibitor. *Chembiochem.* **2013**, *14*, 2263-2267; c) Di  
687 Bussolo, V.; Calvaresi, E. C.; Granchi, C.; Del Bino, L.; Frau, I.; Lang, M. C.; Tuccinardi,  
688 T.; Macchia, M.; Martinelli, A.; Hergenrother, P. J.; Minutolo, F. Synthesis and biological  
689 evaluation of non-glucose glycoconjugated N-hydroxyindole class LDH inhibitors as  
690 anticancer agents. *RSC Adv.* **2015**, *5*, 19944-19954.
- 691 44. Kollman, P. A.; Massova, I.; Reyes, C.; Kuhn, B.; Huo, S.; Chong, L.; Lee, M.; Lee, T.;  
692 Duan, Y.; Wang, W.; Donini, O.; Cieplak, P.; Srinivasan, J.; Case, D. A.; Cheatham, T. E.

- 693 3rd. Calculating structures and free energies of complex molecules: combining molecular  
694 mechanics and continuum models. *Acc. Chem. Res.* **2000**, *33*, 889-897.
- 695 45. Tuccinardi, T.; Granchi, C.; Iegre, J.; Paterni, I.; Bertini, S.; Macchia, M.; Martinelli, A.;  
696 Qian, Y.; Chen, X.; Minutolo, F. Oxime-based inhibitors of glucose transporter 1 displaying  
697 antiproliferative effects in cancer cells. *Bioorg. Med. Chem. Lett.* **2013**, *23*, 6923-6927.
- 698 46. Tuccinardi, T.; Manetti, F.; Schenone, S.; Martinelli, A.; Botta, M. Construction and  
699 validation of a RET TK catalytic domain by homology modeling. *J. Chem. Inf. Model.*  
700 **2007**, *47*, 644-655.
- 701 47. Abdullaev, F.; Riveron-Negrete, L.; Caballero-Ortega, H.; Hernández, J. M.; Perez-Lopez,  
702 I.; Pereda-Miranda, R.; Espinosa-Aguirre, J. Use of in vitro assays to assess the potential  
703 antigenotoxic and cytotoxic effects of saffron (*Crocus sativus* L.). *Toxicol. in vitro* **2003**, *17*,  
704 731-736.
- 705 48. Modagheh, M. -H.; Shahabian, M.; Esmaeili, H. -A.; Rajbai, O.; Hosseinzadeh, H. Safety  
706 evaluation of saffron (*Crocus sativus*) tablets in healthy volunteers. *Phytomedicine* **2008**, *15*,  
707 1032-1037.

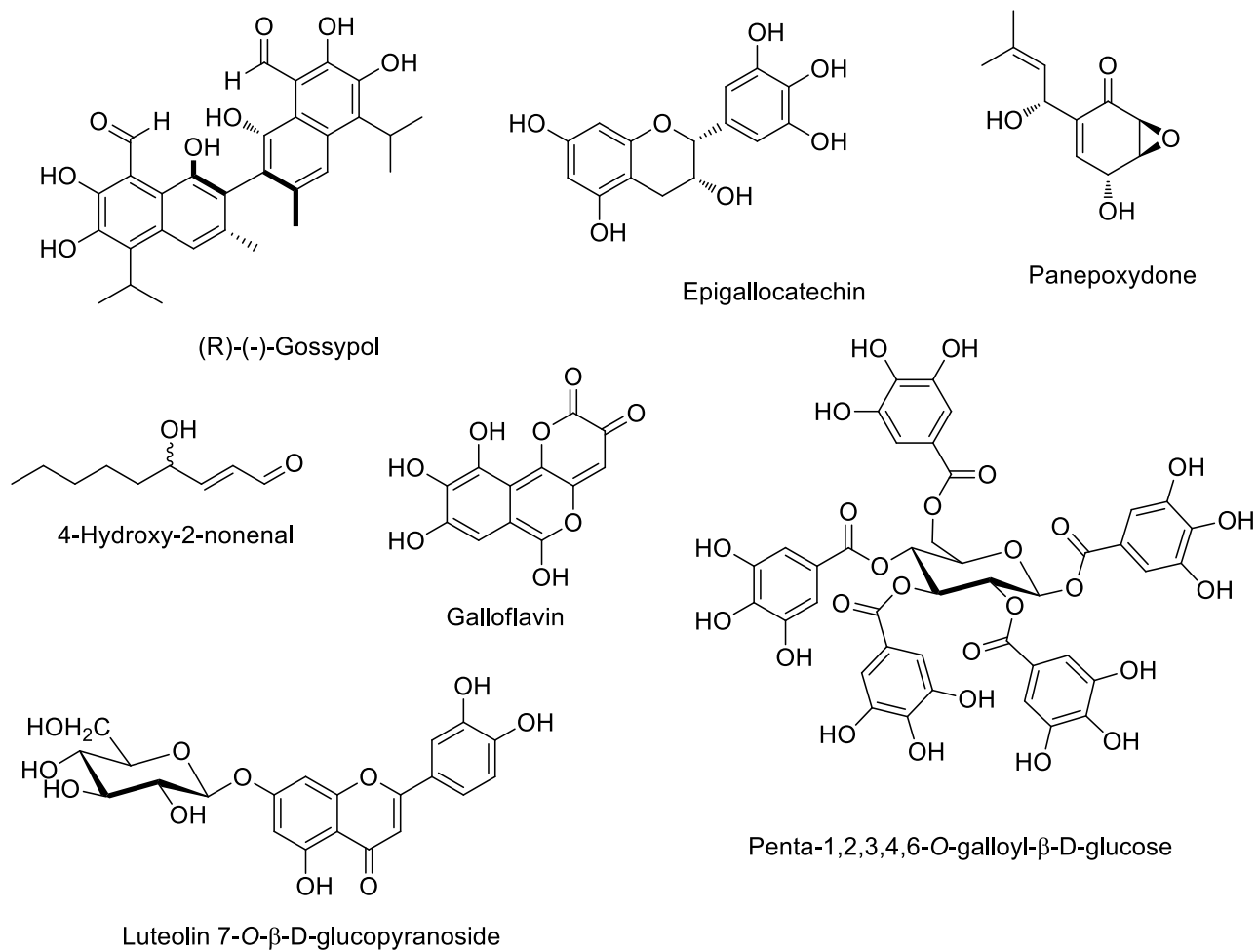
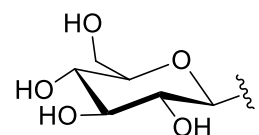
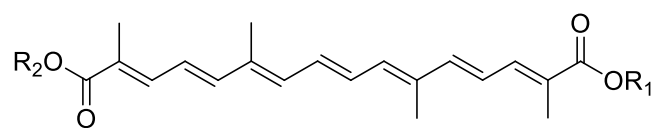


**Figure 1.**



$\beta$ -D-glucosyl

crocins

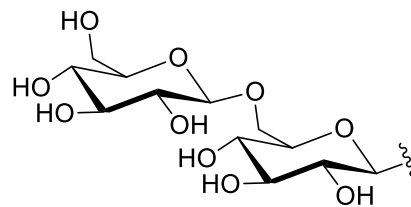
a:  $R_1 = R_2 = \beta$ -D-gentiobiosyl;

b:  $R_1 = \beta$ -D-gentiobiosyl,  $R_2 = \beta$ -D-glucosyl;

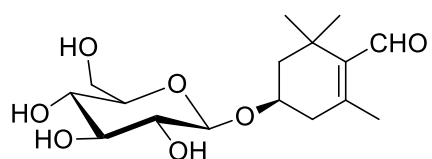
c:  $R_1 = R_2 = \beta$ -D-glucosyl;

d:  $R_1 = \beta$ -D-gentiobiosyl,  $R_2 = H$ ;

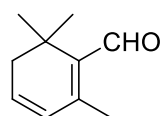
e:  $R_1 = \beta$ -D-glucosyl,  $R_2 = H$ .



$\beta$ -D-gentiobiosyl



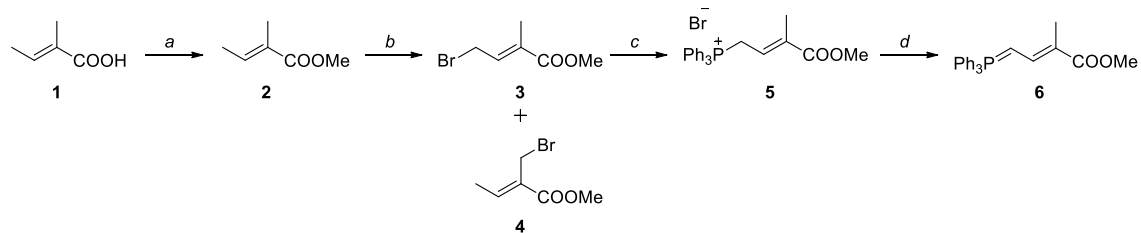
picrocrocin



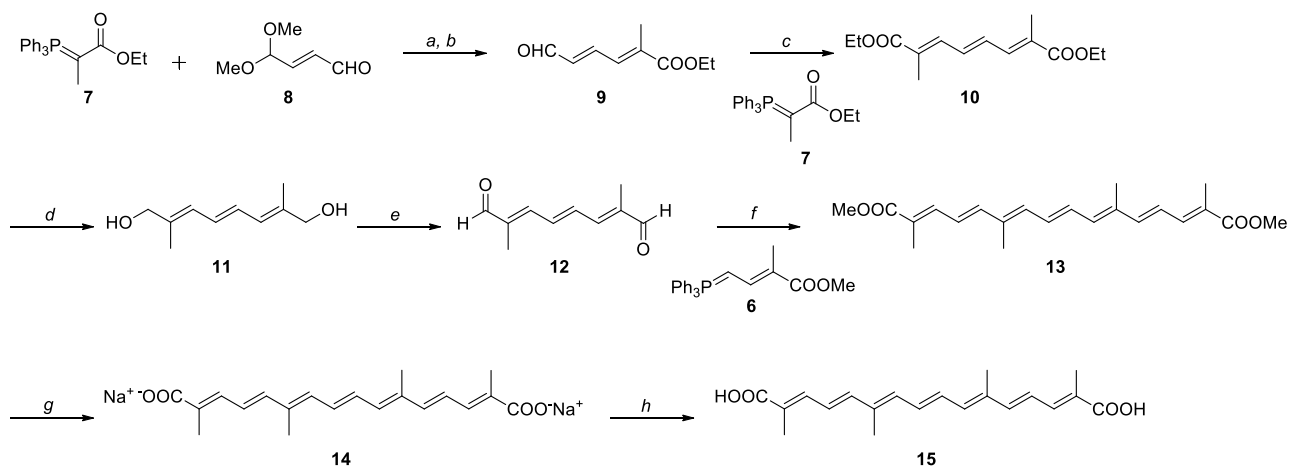
safranal

**Figure 2.**

Part A

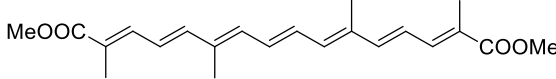
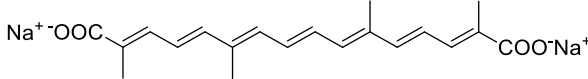
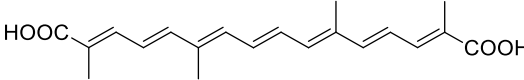
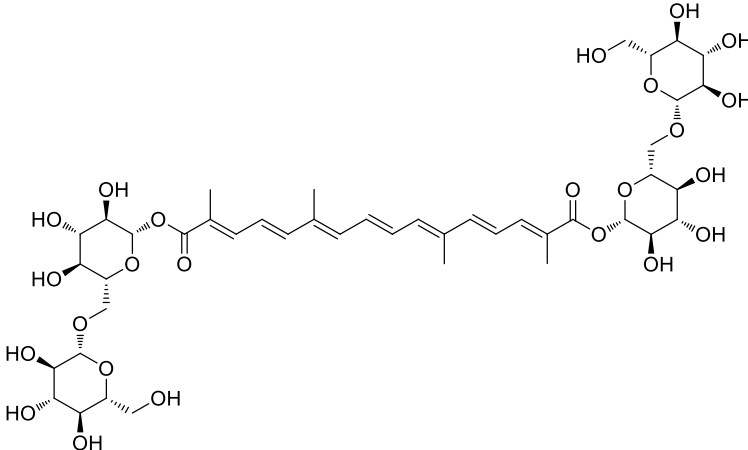
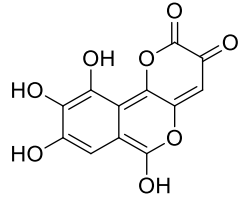


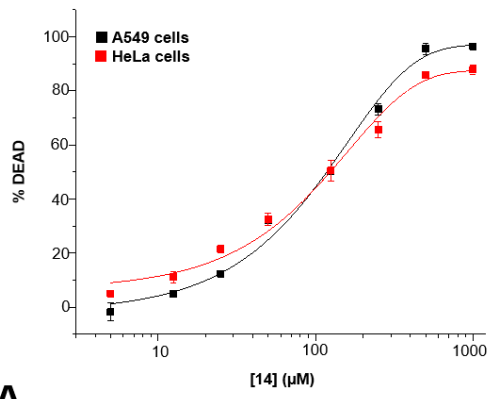
Part B



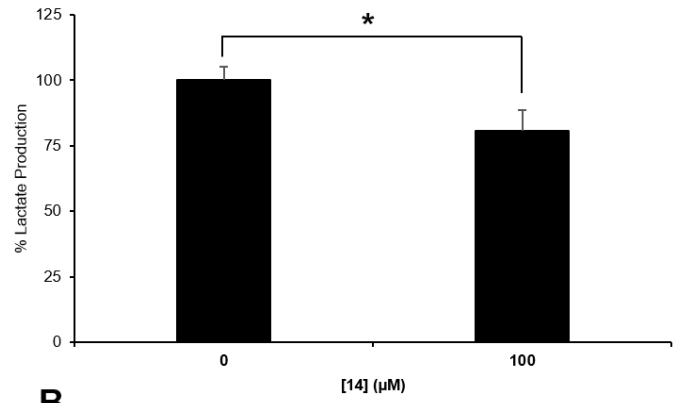
**Scheme 1.**

**Table 1.**

compound	<i>h</i> LDH-5	<i>h</i> LDH-1
	IC <sub>50</sub> , μM	
 <b>13</b>	> 200	> 200
 <b>14</b>	54.9 ± 4.7	> 200
 <b>15</b>	61.9 ± 2.3	> 200
 <b>16</b>	95.7 ± 9.8	59.8 ± 4.2
 <b>Galloflavin</b>	93.2 ± 8.7	123.2 ± 14.2



**A**



**B**

**Figure 3.**

**Table 2.**

	<b>EEL</b>	<b>VDW</b>	<b>ENPOLAR</b>	<b>EPB</b>	<b><math>\Delta</math>PBSA</b>
<b>Pose 1</b>	-208.1	-29.8	-3.8	220.8	-20.9
<b>Pose 2</b>	-255.1	-36.3	-4.2	285.4	-10.2
<b>Pose 3</b>	-279.8	-28.6	-3.9	283.1	-29.2
<b>Pose 4</b>	-218.7	-24.7	-4.1	227.4	-20.1
<b>Pose 5</b>	-147.0	-22.5	-3.3	157.8	-15.0



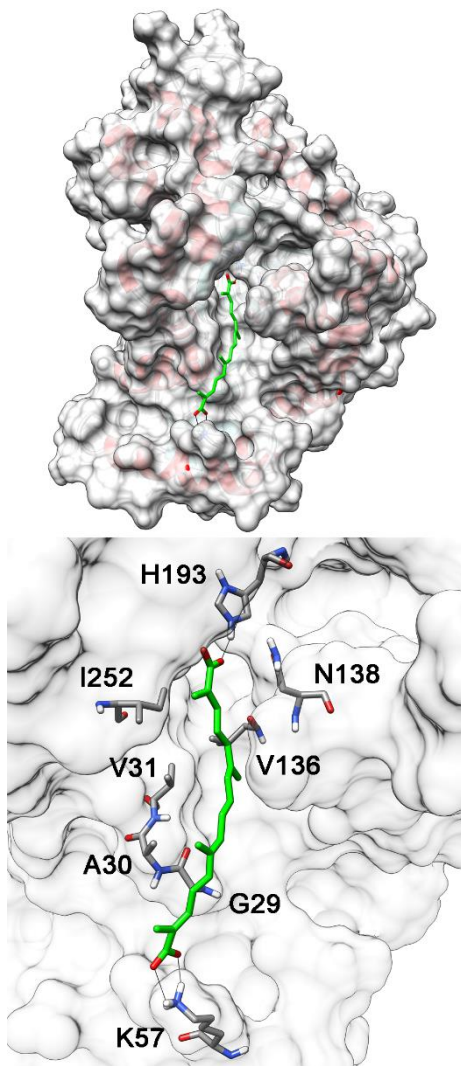


Figure 4.

**Figure 1.** Some representative naturally-derived compounds that inhibit *h*LDH-5.

**Figure 2.** Structures of saffron main metabolites.

**Figure 3.** Panel A: Dose-response curve for compound **14** in A549 and HeLa cells. Panel B: Lactate production inhibition for compound **14** in HeLa cells quantified by GC-MS. % DEAD is less than 28 % in all samples. Mean of three experiments. Error bars show SE (n=3). Statistical analysis was performed using an unpaired, two-tailed student's t test. \*  $p < 0.05$  relative to vehicle control.

**Figure 4.** Putative binding mode of compound **14** into *h*LDH-5. Putative binding pose of the ligand (green) in the binding site and view of the most relevant ligand–receptor interactions.

**Scheme 1.** *Reagents and conditions.* Part A: a)  $\text{H}_2\text{SO}_4$ , MeOH, reflux; b) NBS, BPO,  $\text{CHCl}_3$ , reflux; c)  $\text{PPh}_3$ , toluene, RT; recrystallization from  $\text{CH}_3\text{CN}/\text{AcOEt}$ ; d) 0.5 M NaOH, DCM, RT. Part B: a) DCM, RT; b) Amberlyst 15,  $\text{H}_2\text{O}$ , acetone, RT; c) DCM, RT; d) DIBAL-H, an. hexane, -78 °C to -20 °C; e) activated  $\text{MnO}_2$ , acetone, 0 °C to RT; f) toluene, reflux; g) aq. NaOH, MeOH, reflux; h)  $\text{H}_3\text{PO}_4$ .

**Table 1.** Enzyme inhibition potencies.

**Table 2.** MM-PBSA results for the five different *h*LDH-5-compound **14** complexes.  $\Delta\text{PBSA}$  is the sum of the electrostatic (EEL) and van der Waals (VDW), as well as polar (EPB) and non-polar (ENPOLAR) solvation free energy. Data are expressed as kcal/mol.

